

Exchange in multi-defect semiconductor clusters: assessment of ‘control-qubit’ architectures

W. Wu, P. T. Greenland, and A. J. Fisher*

*UCL Department of Physics and Astronomy and London Centre for Nanotechnology,
University College London, Gower Street, London WC1E 6BT*

(Dated: April 24, 2022)

We present a variational method to calculate the exchange interactions among donor clusters in a semiconductor. Such clusters are candidates for a so-called control-qubit architecture for quantum information, where the effective exchange coupling between two atoms is controlled by the electronic state of a third. We use a combination of the effective-mass approximation and the quantum defect method; our variational *ansatz* is particularly suited to cases where an excited state of one of the donors (control) is partially delocalised over several different centres, forming an analogue of an extended molecular orbital. Our method allows calculations of the “on/off” ratios of exchange interactions in such cases. We compare exchange interactions when the control is in the “on” and “off” states, and find that both the magnitude and sign of the exchange interactions may be changed. To rationalize the sign-change, we carry out a simple Green’s function perturbation-theory calculation. This simple model qualitatively explains the sign change and illustrates its origins both in ring-exchange processes and in the delocalization of the control electron. We also compute probability distributions for the coupling strengths over the ensemble of clusters, and show that excitation of the control causes narrowing of the distributions along with shifts to larger magnitudes and from anti-ferromagnetic to ferromagnetic coupling.

PACS numbers: 03.67.Lx, 71.55.Cn

I. INTRODUCTION

Proposed silicon-based quantum computer architectures [1, 2] have attracted attention because of their promise of scalability and their potential for integration with existing CMOS architectures. Localized spins in Si are one very promising means to represent quantum information: spin- $\frac{1}{2}$ objects are natural two-level systems, so they may naturally be used to embody a qubit. Furthermore, in pure Si, electron spins are associated only with defects and so are naturally isolated.

Implementing general quantum gates requires one to produce entangling interactions between localized spins in order to evolve these spin states. Previous approaches to controlling these interactions [1] required gate electrodes positioned near to specific highly polarizable (therefore shallow) donors; such defects are however readily ionized except at low temperatures, and have spin-lattice relaxation times declining rapidly with temperature because of the presence of spin-flip Raman transitions [3]. In addition the presence of the gates may introduce significant additional decoherence through their interaction with the polarizable defects, as well as posing formidable difficulties in the accurate positioning of the defects relative to the electrodes [4, 5].

An alternative scheme for controlling the interactions, which avoids the need for electrodes, was proposed in [6]. Quantum bits are encoded into electron spins of *deep* donors, with the advantages of lower ionization prob-

abilities and much longer spin-lattice relaxation times [3]. Interactions are controlled, not by gates, but by local electronic excitations [6]. Specifically, let (A,B) be two such deep donor atoms. Their spacing should be sufficiently large that the ground-state interaction between donor spins is small (ideally negligible). Controlled optical excitation [7, 8] can promote a “control” electron from a nearby impurity C into an excited state that is to some extent delocalized across A, B and C. In this excited state, there is expected to be an effective exchange interaction induced between the two qubit spins. Qubit-qubit interactions are therefore switched on by optical excitation and off by (stimulated) de-excitation of the control electron. Note that in this picture the electronic excitation is real, not virtual, in contrast to other schemes that have been proposed to couple quantum dots in semiconductors [9]; this has the advantage that the wavelength variations arising from the inhomogeneity of the sample can be exploited to address it on scales much smaller than the optical wavelength [6], while leaving the control spins unentangled with the qubits if the operating parameters are chosen carefully [10].

To build a quantitative model of these processes, we need to understand how the exchange interactions depend on the different types of donors involved (deep or shallow), their separations, the presence or otherwise of electronic excitations, and the extent of delocalization of these excitations. Exchange interactions between pairs of hydrogenic impurities in semiconductors have been studied for many years [2, 11, 12, 13, 14, 15, 16], and we recently showed how these approaches could be easily generalized to pairs of deep donors with an arbitrary binding energy [17] using a simple quantum-defect approach.

*Electronic address: andrew.fisher@ucl.ac.uk

The exchange among defect clusters has been much less studied, except where the clusters strongly influence the bulk magnetic properties, as in for example (Ga,Mn)As [18], although the general importance of multi-centre interactions in determining exchange properties has been known for many years, notably in the context of solid ^3He [19]. Their potential significance for quantum information processing with electron spins was pointed out more recently [20, 21, 22]; however this work focussed on harmonic potential wells in highly symmetric arrangements. Deviations from the classic form of Heisenberg exchange have also been discussed [23] in the context of multiple quantum dots, and are important when the dots are very strongly coupled or in very large magnetic fields.

We focus on a different aspect of the problem, and present a simple variational calculation designed to capture the essential physics: the presence of deep and shallow impurities, a range of geometries, and the possibility of electron delocalization in the excited state. We adopt a reference model in which the qubits are deep donors (for example, Bi:Si) while the control atom is a shallow donor (e.g. P:Si), and treat it in configurations where the control is equidistant from the qubits. This remaining symmetry simplifies the calculations while enabling us to study separately the effects of qubit-qubit and control-qubit separations. Our basic model can be thought of as a multi-spin generalization of the well-known Heitler-London approach [24, 25] to the exchange interactions in the hydrogen molecule. Although this approximation fails at very large separations [25] because of the neglect of correlation terms, it is very accurate over the physically interesting range of separations up to about 12 effective Bohr radii, beyond which dipolar interactions anyway become dominant [17]. We also show that we can rationalize our main results using simple perturbation theory.

The remainder of the paper is organized as follows. In §II, we introduce our methods and the basis used to describe the wave functions of deep and shallow donors. In the §III, we present our results for a range of qubit and control positions. In §IV we discuss the results and show how they can be related to the so-called kinetic exchange arising from multi-centre interactions by using perturbation theory; then in §V we show how the distributions of exchange that would be probed by bulk measurements are influenced by the properties of the defect clusters and their degree of excitation. We do not address the optical excitation and de-excitation processes; these will be discussed in a forthcoming paper [26].

II. METHOD OF CALCULATION

A. Geometry and representation of the solid

Let \vec{R}_C , \vec{R}_A , and \vec{R}_B be the position vectors of the control nucleus, the first qubit nucleus, and the second qubit nucleus respectively. We take the distance between the

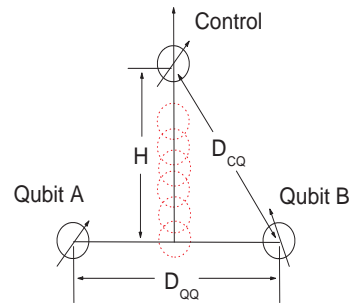


FIG. 1: The geometry used for the three-atom system.

qubits as $|\vec{R}_A - \vec{R}_B| = D_{QQ}$; for reasons that will become clear below, we take the triangle formed by our three atoms to be isosceles, so that a reflection plane exists bisecting the two qubit atoms. Let the height of this triangle be H ; the control atom is then equidistant from both qubits and $|\vec{R}_C - \vec{R}_A| = |\vec{R}_C - \vec{R}_B| = \sqrt{H^2 + (D/2)^2} \equiv D_{CQ}$. This geometry is sketched in Figure 1.

We treat the three donors within isotropic, single-band effective-mass theory [27, 28], introducing quantum defect corrections [30] where necessary to modify the binding energies. This is the simplest model that enables us to concentrate on the mutual interaction of the three donors, and we have recently shown [17] that it is able to describe the exchange between donor pairs with arbitrary binding energy. However, it does neglect the valley degeneracy of the silicon conduction band, which in reality contributes a degeneracy of the donor states and corresponding interference terms in the exchange [12, 13, 14]. In common with other recent treatments we do not treat the conduction-band anisotropy directly, instead capturing its main effects by choosing an appropriate average effective mass.

Within the effective-mass model, the Hamiltonian of this three-electron system is

$$\hat{H} = \sum_i \hat{h}_i + \frac{1}{2} \sum_{i \neq j} \frac{1}{|\vec{r}_i - \vec{r}_j|}, \quad (1)$$

where

$$\hat{h}_i = -\frac{\nabla_i^2}{2} - \frac{Z_C}{|\vec{r}_i - \vec{R}_C|} - \frac{Z_A}{|\vec{r}_i - \vec{R}_A|} - \frac{Z_B}{|\vec{r}_i - \vec{R}_B|}. \quad (2)$$

Here \vec{r}_i labels the coordinate of electron i , and Z_C , Z_A , and Z_B are respectively the charges of the control nucleus, the first nucleus, and the second nucleus. We consider single donors and treat only the outermost electron explicitly and therefore take $Z_C = Z_A = Z_B = 1$. Since we neglect spin-orbit coupling and dipole-dipole interactions, the system Hamiltonian contains no explicit spin operators and the total spin S is a good quantum number.

We use scaled atomic units throughout: we take a mean (directionally averaged) conduction-band effective

mass for Si of $m^* = 0.33m_e$ (where m_e is the free electron mass), and a relative permittivity $\epsilon_r = 11.4$, leading to an effective Bohr radius about $a_0^* = 1.94$ nm and an effective Hartree $\text{Ha}^* = 33.48$ meV [29].

B. Single-centre basis functions

We suppose there is a single important orbital ϕ_C at the control site (whose nature changes depending on the degree of excitation of the control) and two important orbitals at each qubit site: ground-state orbitals χ_i (where $i \in \{A, B\}$) which accommodate the qubit electrons, and excited orbitals ϕ_i which allow for delocalization of the control electron. In this paper we will assume that all of these states have s symmetry, and use quantum-defect methods to represent their radial parts.

We make this choice so that we can work equally well with deep and shallow impurities (deep donors are especially promising for QIP applications [6]), and still have functions that are described by effective mass theory far from the defects. Bebb [30] showed how quantum defect methods could be used to obtain good approximate wave functions in the region outside the impurity ion core, using only a knowledge of the energy eigenvalues. In this region, where the potential approaches $u(r) \sim -1/r$, the radial Schrödinger equation is

$$\left(\frac{1}{2} \frac{d^2}{dr^2} - \frac{l(l+1)}{2r^2} - u(r) - \frac{1}{2\nu^2}\right)P(r) = 0, \quad (3)$$

where $-1/2\nu^2$ is just ϵ , the observed energy level. It is conventional to write $\nu = n - \mu(\epsilon_n)$, where n is the usual principal quantum number, μ is the quantum defect, and

$$\epsilon_n = \frac{\text{Ha}^*}{2\nu^2} = \frac{\text{Ha}^*}{2(n - \mu(\epsilon_n))^2}. \quad (4)$$

where Ha^* is the effective Hartree.

The solution of (3) that is regular at infinity is $P_{\nu,l}(r)$, but if $\mu \neq 0$ this solution diverges at the origin if the

potential remains $1/r$ down to short distances. We must therefore suppose that the short-range deviation of the potential from the Coulomb form is such that the true solution is indeed regular at the origin; the solution $P_{\nu,l}(r)$ is only valid outside the core. In principle one could determine the entire eigenfunction using some form of central cell correction [31, 32, 33]. However for our purposes the asymptotic form is sufficient to calculate the exchange interactions when the donor separations are large.

The normalized quantum defect wavefunction is

$$P_{\nu,l}(r) = N_{\nu,l} W_{\nu,l+\frac{1}{2}}(2r/\nu). \quad (5)$$

Here W is a Whittaker function [36], defined in terms of hypergeometric functions U by

$$W_{\kappa,\mu}(z) = e^{-z/2} z^{1/2+\mu} U\left(\frac{1}{2} - \kappa + \mu, 1 + 2\mu, z\right). \quad (6)$$

The approximate normalization constant $N(\nu, l)$ is given by [30].

In this paper we take $\mu = 0$ (and hence $\nu = 1, 2, \dots$) for shallow (control) donors, and $\mu = 0.3$ (hence $\nu = 0.7, 1.7, \dots$) for the more deeply bound qubit states.

C. Variational method

We make a simple variational assumption for the wave function of the control electron, writing the corresponding one-electron state as

$$\psi_C = \alpha\phi_C + \beta\phi_A + \gamma\phi_B. \quad (7)$$

Although this is a very simple choice, and will not reflect the full complexity of the problem, it does give the control electron variational freedom to adjust between the extremes of being localized entirely on the control atom, or entirely on a "molecular" excited state of the qubit atoms A and B .

We then construct a three-electron variational function in the form

$$\Psi_{total}^Q(x_1, x_2, x_3) = \hat{A}[\psi_C(\vec{r}_1)(\chi_A(\vec{r}_2)\chi_B(\vec{r}_3) - \chi_A(\vec{r}_3)\chi_B(\vec{r}_2))Q] \quad (8)$$

$$\Psi_{total}^{D_1}(x_1, x_2, x_3) = \hat{A}[\psi_C(\vec{r}_1)(\chi_A(\vec{r}_2)\chi_B(\vec{r}_3) - \chi_A(\vec{r}_3)\chi_B(\vec{r}_2))D_1] \quad (9)$$

$$\Psi_{total}^{D_0}(x_1, x_2, x_3) = \hat{A}[\psi_C(\vec{r}_1)(\chi_A(\vec{r}_2)\chi_B(\vec{r}_3) + \chi_A(\vec{r}_3)\chi_B(\vec{r}_2))D_0], \quad (10)$$

where Q refers to the quartet (total spin $S = 3/2$), D_1 refers the doublet (total spin $S = 1/2$) constructed from the triplet state of the qubits, and D_0 refers to the doublet (total spin $S = 1/2$) constructed from the singlet state of the qubits. \hat{A} is the antisymmetrizing operator. The existence of a plane of symmetry in our assumed ge-

ometry means that the functions $\Psi_{total}^{D_1}$ and $\Psi_{total}^{D_0}$, which have opposite parities with respect to the exchange of the qubits, cannot mix and can be varied independently.

Note that, in constructing the above function, we have neglected high-energy 'ionic' configurations in which both qubit electrons reside on the same atom. We have also neglected correlations between the control electron and

the qubit electrons.

We now perform a variational calculation using undetermined multiplier methods to minimize the expectation values of the system Hamiltonian:

$$\frac{\partial E_i}{\partial \alpha} + \lambda \frac{\partial S_i}{\partial \alpha} = 0 \quad (11)$$

$$\frac{\partial E_i}{\partial \beta} + \lambda \frac{\partial S_i}{\partial \beta} = 0 \quad (12)$$

$$\frac{\partial E_i}{\partial \gamma} + \lambda \frac{\partial S_i}{\partial \gamma} = 0, \quad (13)$$

$$(14)$$

where $i \in \{Q, D_1, D_0\}$, λ is the undetermined multiplier, $E_i = \langle \Psi_i | \hat{H} | \Psi_i \rangle$ and $S_i = \langle \Psi_i | \Psi_i \rangle$.

D. Extraction of the spin Hamiltonian

Once we have the energies (E_Q, E_{D_1}, E_{D_0}), of the spin states, we can calculate the exchange constants. Provided spin-orbit coupling is negligible, the three-electron spin Hamiltonian in zero external field must take the form

$$\hat{H}_{eff} = J_{CQA} \vec{s}_A \cdot \vec{s}_C + J_{CQB} \vec{s}_B \cdot \vec{s}_C + J_{QQ} \vec{s}_A \cdot \vec{s}_B, \quad (15)$$

because this is the only form which is (i) invariant under simultaneous rotation of all the spins and (ii) even under time-reversal. Furthermore, atoms A and B are equivalent in our calculation, so $J_{CQA} = J_{CQB} = J_{CQ}$. We can then calculate the exchange constants in the effective Hamiltonian from the eigenvalues and eigenstates. As explained in §II C and Appendix A, the doublet states are distinguished by the ‘intermediate’ angular momentum of the qubit spins (A and B); once these states have been identified, the parameters in equation (15) can be extracted to give

$$\begin{aligned} J_{QQ} &= -\frac{4}{3} E_{D_0} \\ J_{CQ} &= 2 \left(E_Q - \frac{J_{QQ}}{4} \right) \end{aligned} \quad (16)$$

where the zero of energy is chosen to be the weighted mean of the spin energies, so the spin Hamiltonian is traceless. Note that, with the sign convention adopted in setting up the spin Hamiltonian (15), positive couplings J correspond to antiferromagnetic interactions.

III. VARIATIONAL CALCULATION: RESULTS

In Figures 2 and 3 we show respectively the control-qubit coupling J_{CQ} and the qubit-qubit coupling J_{QQ} , as the qubit-qubit distance D_{QQ} varies from 1 to $12a_0^*$ and the height H of the triangle formed by the qubits and control varies from 0 to $10a_0^*$. In these and subsequent figures the geometry is as shown in Figure 1, the

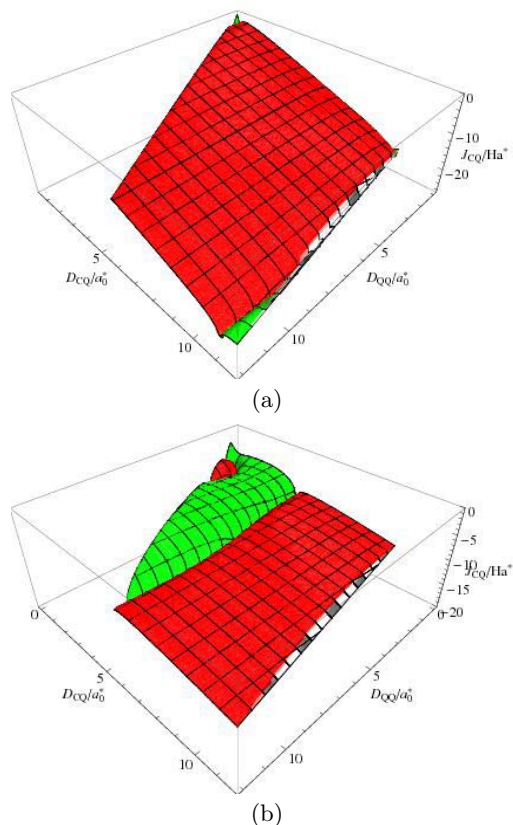


FIG. 2: (Colour online.) The control-qubit exchange coupling J_{CQ} (logarithmic scale) for the case where a shallow-donor control and deep-donor qubits ($\nu = 0.7$) are in the spatial configuration shown in Figure 1 as a function of qubit donor distance D_{QQ} and the qubit-control distance D_{CQ} . (a) Control is in the ground state ($\nu = 1.0$); (b) control in the excited state ($\nu = 2.0$). The sign of exchange coupling is coded in color; red: positive (antiferromagnetic) and green: negative (ferromagnetic). D_{QQ} varies from 1.0 to $12.0a_0^*$; H varies from 0 to $10a_0^*$. Note that the vertical scales in the two plots are the same.

two qubits are deep donors, and the shallow control is either (a) in the ground state ($\nu = 1$) or (b) in the excited state ($\nu = 2$). All results are shown as a function of D_{QQ} and the qubit-control distance $D_{CQ} = \sqrt{H^2 + D_{QQ}^2}/4$; the constraint $D_{CQ} \geq D_{QQ}/2$ is therefore enforced by our geometry.

It is immediately evident from Figure 2(a) that even with the control in its ground state, J_{CQ} depends (weakly) on D_{QQ} as well as (strongly) on D_{CQ} . Throughout most of the region J_{CQ} is positive (antiferromagnetic), as would be expected for a two-electron system [34], although in some small regions it becomes negative (ferromagnetic). Figure 2(b), where the control is in the excited state, shows very different behaviour: now the effective coupling is much larger and decays much more slowly (as we would expect) but is also ferromagnetic over a significant part of parameter space (which is more surprising). We will see below that this change is related

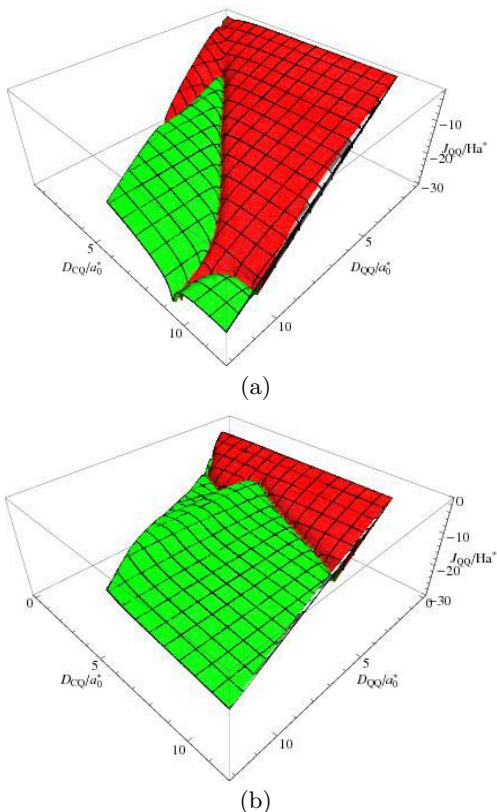


FIG. 3: (Colour online.) The qubit-qubit exchange coupling J_{QQ} (logarithmic scale) for the case where a shallow-donor control and deep-donor qubits ($\nu = 0.7$) are in the spatial configuration shown in Figure 1 as a function of qubit donor distance D_{QQ} and qubit-control distance D_{CQ} . (a) control is in the ground state ($\nu = 1.0$); (b) control in the excited state ($\nu = 2.0$). The sign of exchange coupling is coded in color; red: positive (antiferromagnetic) and green: negative (ferromagnetic). D_{QQ} varies from 1.0 to $12.0a_0^*$; H varies from 0 to $10a_0^*$. Note that the vertical scales in the two plots are the same, and that the constraint $D_{CQ} \geq D_{QQ}$ is enforced by our geometry.

to a change in the spatial location of the control electron, as it becomes delocalized over the three centres.

Similar cooperative behaviour is evident in the behaviour of the qubit-qubit coupling J_{QQ} , which displays a more complex structure than the exponential decrease with D_{QQ} that one might naively expect. Figure 3(a) shows that the coupling is predominantly exponential in D_{QQ} only when $D_{QQ} \ll D_{CQ}$, but this behaviour changes when the control atom becomes situated close to the midpoint of AB. For $D_{QQ} \geq D_{CQ}$, J_{QQ} is negative (ferromagnetic) and strongly dependent on D_{CQ} as well as D_{QQ} ; this contrasts with the two-electron case [34], where J_{QQ} should be always positive (antiferromagnetic). This illustrates that even in the ground state the shallow-donor control electron can cause a significant perturbation to the originally relatively weak exchange couplings in the two-qubit system.

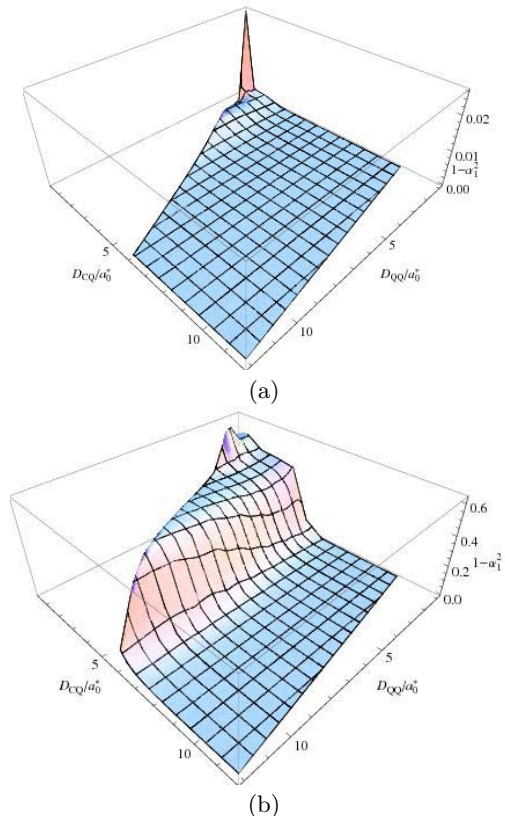


FIG. 4: (Colour online.) The probability $1 - \alpha_1^2$ of finding the control donor electron on the qubit sites for the case where a shallow-donor control and deep-donor qubits ($\nu = 0.7$) are in the spatial configuration shown in Figure 1 as a function of qubit donor distance D_{QQ} and qubit-control distance D_{CQ} . (a) control is in the ground state ($\nu = 1.0$); (b) control in the excited state ($\nu = 2.0$). D_{QQ} varies from 1.0 to $12.0a_0^*$; H varies from 0 to $10a_0^*$.

The transitions between different regimes can be largely understood from Figure 4, which shows the variation of $1 - |\alpha|^2$ and hence of the probability (in the Mulliken sense) that the control electron is located on the qubit sites. We see that $|\alpha|^2 \approx 1$ throughout, except in the excited state when the control is relatively close to the qubits. In that case $|\alpha|^2 \ll 1$ and the control state hybridizes strongly with the virtual orbitals on the qubit atoms. In this case the physics of the exchange is dominated by local interactions between the control and qubit spins similar to those in the $1s2s$ excited state of He, where there is a ferromagnetic exchange splitting of $6,422 \text{ cm}^{-1}$ or 0.80 eV [37].

We focus on how the control electron alters J_{QQ} and plot the ratio of this quantity with and without the control present in Figure 5. As expected, when the control is very far away from qubits ($D_{CQ} \gg D_{QQ}$), the ratio is close to unity. When this condition is not satisfied (i.e., for $D_{CQ} \lesssim D_{QQ}$), J_{QQ} is strongly modified and (over a large part of the region) ferromagnetic. In the excited state (Figure 5(b)) the coupling is enhanced and ferro-

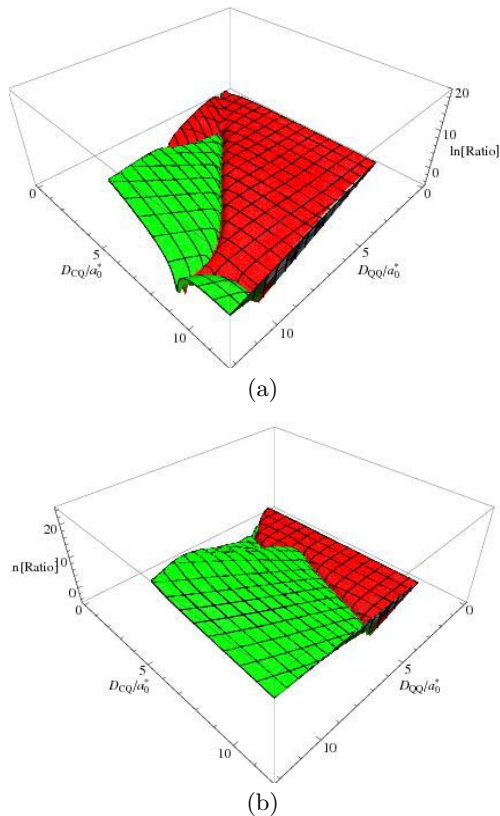


FIG. 5: (Colour online.) The ratio (logarithmic scale) of the qubit-qubit exchange couplings J_{QQ} for two deep-donor qubits ($\nu = 0.7$) with and without a shallow-donor control. The spatial configuration is as shown in Figure 1; results are shown as a function of the qubit-qubit distance D_{QQ} and the qubit-control distance D_{CQ} . In (a) the control is in the ground state ($\nu = 1.0$); in (b) the control in the excited state ($\nu = 2.0$). The sign of the ratio is coded in color; red: positive (antiferromagnetic interaction in presence of control), and green: negative (ferromagnetic). In the absence of the control, the interaction is always antiferromagnetic.

magnetic almost everywhere, unless $D_{CQ} \gg D_{QQ}$. We will show in §IV that the ferromagnetic interactions are a consequence of ring exchange among the three atoms.

Finally, in Figure 6, we focus on the changes brought about by excitation (the ‘on/off ratios’ of the exchange). As would be expected, excitation almost always increases the magnitude of the exchange; Figure 6(a) (for J_{CQ}) shows that this effect is largest for large D_{QQ} and moderate D_{CQ} , although there is a relatively complicated behaviour of the sign of the ratio as a result of the differing crossovers between ferromagnetic and antiferromagnetic exchange in the ground and excited states (Figure 3). Figure 6(b) (for J_{QQ}) shows a simpler pattern: the on/off ratio increases with D_{CQ} and remains only weakly dependent on D_{QQ} .

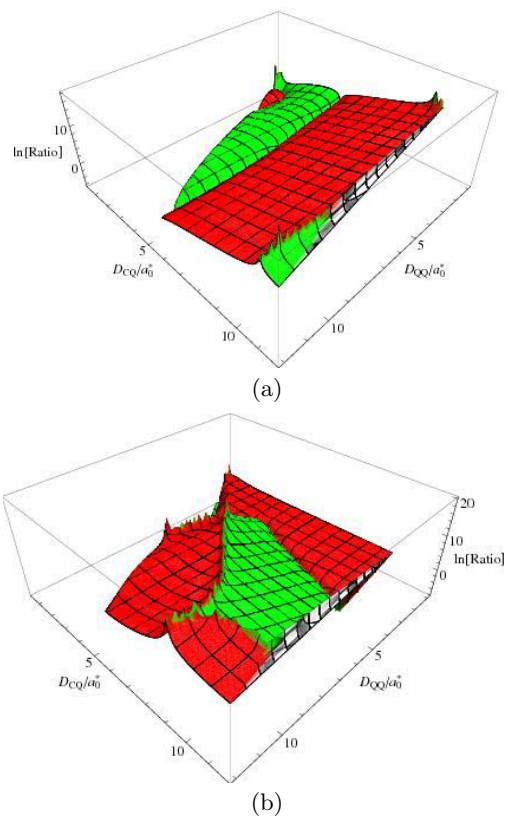


FIG. 6: (Colour online.) The ratios J^e/J^g (logarithmic scale) of the exchange interactions for the control excited (J^e , with $\nu = 2.0$) to control-unexcited (J^g , with $\nu = 1.0$) for a shallow-donor control and deep-donor qubits: (a) control-qubit exchange J_{CQ} , (b) qubit-qubit exchange J_{QQ} . The sign of the ratio is coded in color: red: positive and green: negative.

IV. RING-EXCHANGE MODEL

A. Multi-center ring exchange

In this section, we present an alternative calculation of the exchange constants by using Green’s-function perturbation theory. This approach has the advantage that it gives a clear picture of the origins of different contributions to the exchange. In particular it allows us to understand the origin of the ferromagnetism of J_{QQ} in §III: owing to the presence of the shallow control atom, multi-body ring exchange process [19] become possible and higher-order ring exchange process (which can be ferromagnetic) may dominate over the direct second-order exchange between the qubits provided $D_{CQ} \ll D_{QQ}$.

The essential physics of our system is similar to that in solid ^3He [19], despite the very different chemical nature of the material. In solid ^3He , two-body exchange always leads to a Heisenberg Hamiltonian with antiferromagnetic exchange (Figure 7a), while three-body ring exchange (Figure 7b) and four-body ring exchange (Figure 7c) lead respectively to ferromagnetic and anti-

ferromagnetic contributions.

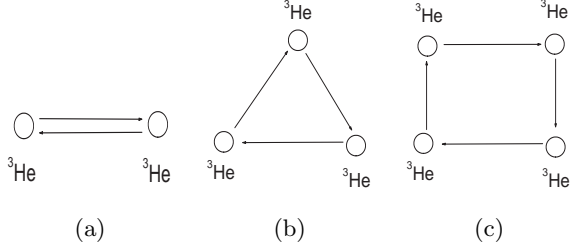


FIG. 7: Schematic view of possible exchange couplings between helium atoms in solid ^3He : (a) conventional two-body exchange (antiferromagnetic); (b) three-body ring exchange (ferromagnetic); (c) Four-body ring exchange (antiferromagnetic).

As in the solid ^3He system we need to include third-order and fourth-order processes (Figure 8) in our Green's function perturbation theory calculation in order to capture these effects of control atom.

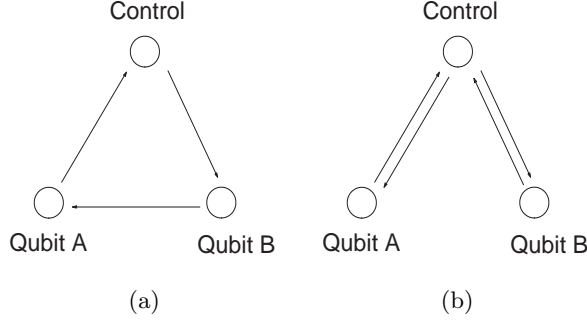


FIG. 8: Schematic view of multi-centre exchange processes in the control-qubit system: (a) third-order exchange scheme; (b) fourth-order exchange scheme.

B. Green's functions time-independent perturbation theory

Suppose the Hamiltonian for a system can be separated into an unperturbed part of H_0 , and a perturbation V ; $H = H_0 + V$. We assume the eigenvalues and eigenfunctions of H_0 are easily obtained. Green's functions $G_0(z)$ and $G(z)$ corresponding to H_0 and H , respectively, are $G_0(z) = (z - H_0)^{-1}$, and $G(z) = (z - H)^{-1}$. G and G_0 are connected by the Dyson equation

$$G(z) = [1 - G_0(z)V]^{-1}G_0(z) \quad (17)$$

$$= G_0 + G_0VG_0 + G_0VG_0VG_0 + \dots, \quad (18)$$

and the effective Hamiltonian which can mix a particular subset \mathcal{S} of the eigenstates of \hat{H}_0 is

$$\begin{aligned} \Delta\hat{H}_{\text{eff}}(z) &= \hat{P}\hat{V}\hat{P} + \hat{P}V\hat{Q}\hat{G}_0(z)\hat{Q}V\hat{P} \\ &+ \hat{P}V\hat{Q}\hat{G}_0(z)\hat{Q}V\hat{Q}\hat{G}_0(z)\hat{Q}V\hat{P} + \dots \end{aligned} \quad (19)$$

where $\hat{Q} = \hat{1} - \hat{P}$, \hat{P} is the projection operator onto the set \mathcal{S} , and the 1st-, 2nd-, 3rd-order... energy shifts are adumbrated on the right-hand side of equation (19). In this formula, $\Delta\hat{H}_{\text{eff}}$ depends on z , which should therefore be chosen to correspond to the energy of the states \mathcal{S} . In the next section, we will show how we use Green's function perturbation theory to extract the exchange constants.

C. Simple model of the three-centre problem

From Figure 4 we see that the control electron resides on the control atom over the majority of parameter space; nevertheless, Figure 3 shows J_{QQ} is ferromagnetic for much of this region. Therefore for simplicity we ignore the donor excited states, retaining only one orbital per site. We consider as parts of \hat{H}_0 all processes which do not transfer charge between centres (both single-electron terms and Coulomb interactions within one atom, and Coulomb interactions between different centres); the perturbation V then contains hopping operators that transfer electrons between centres. Equation (17) then has a simple interpretation reflected in (19): G_0 gives the propagation of uncoupled atoms, while \hat{V} exchanges electrons between those atoms.

Then we carry out our calculation in the following steps. First, we select a particular eigenvalue of the z -component of the total spin S_z (in the following discussion, we choose $S_z = \frac{1}{2}$) (S_z is a good quantum number since we ignore the spin-orbit coupling). Next we enumerate all the possible configurations for this S_z . (For $S_z = \frac{1}{2}$ the nine configurations are shown in Figure (9).) We choose which of these states we will retain as our set \mathcal{S} ; typically, this is the low-energy subspace with one electron per donor, so that Coulomb interactions are minimized. Next we construct the matrices of G_0 and V based on all these possible states (see §IV B), and use these matrices to derive 2nd-, 3rd-, and 4th-order terms in ΔH_{eff} according to equation (19). (We suppose the higher terms are negligible.) Finally, as in the variational calculation (§II C), we identify the values J_{CQ} and J_{QQ} by comparing the effective Hamiltonian in the last step with the Heisenberg Hamiltonian (15).

D. Perturbation theory calculation

1. The unperturbed hamiltonian H_0 .

We take for H_0 a simple extended Hubbard-type Hamiltonian:

$$\begin{aligned} \hat{H}_0 &= E_C\hat{n}_C + E_Q(\hat{n}_A + \hat{n}_B) \\ &+ U_C\hat{n}_{C\uparrow}\hat{n}_{C\downarrow} + U_Q(\hat{n}_{A\uparrow}\hat{n}_{A\downarrow} + \hat{n}_{B\uparrow}\hat{n}_{B\downarrow}) \\ &+ V_{CQ}\hat{n}_A\hat{n}_B + V_{CQ}\hat{n}_C(\hat{n}_A + \hat{n}_B). \end{aligned} \quad (20)$$

Here E_C and E_Q are the single-particle energies of the control and qubit atoms, U_C and U_Q are on-site Coulomb

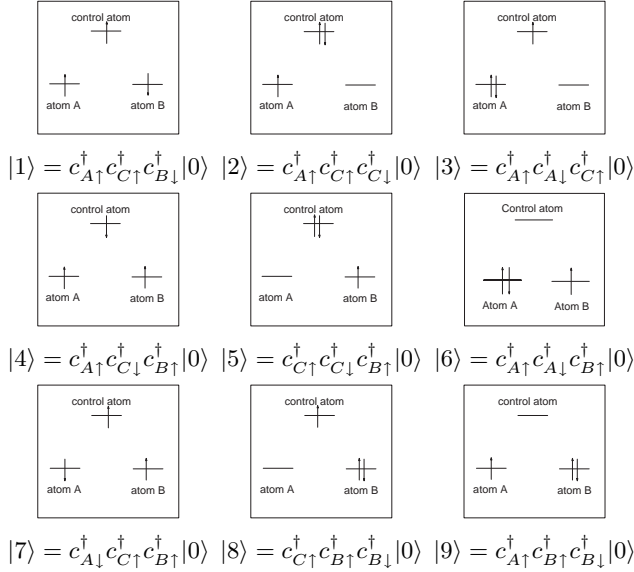


FIG. 9: Schematic of nine possible states according to the calculation procedure in §IV C. We define second-quantizing operators: $c_{A\sigma}^\dagger$, $c_{A\sigma}$, $c_{C\sigma}^\dagger$, $c_{C\sigma}$, $c_{B\sigma}^\dagger$, $c_{B\sigma}$, where σ is \uparrow or \downarrow , and $c_{A\sigma}^\dagger$ is electron-creating operator on the state of qubit A, etc.

interactions in the control and qubit, and V_{QQ} and V_{CQ} are respectively Coulomb interactions between electrons in the two qubit sites, and between electrons in the control and qubit sites. $\hat{n}_{i\sigma}$ is the number operator for electrons with spin σ on site i , and $\hat{n}_i = \hat{n}_{i\uparrow} + \hat{n}_{i\downarrow}$.

We take for the perturbation \hat{V} the hopping terms that transfer electrons respectively between the control atom and the qubits, and from qubit to qubit. If we assume the corresponding amplitudes t_{CQ} , t_{QQ} are real, then we can write

$$\hat{V} = \sum_{\sigma} [t_{CQ}(\hat{c}_{A\sigma}^\dagger \hat{c}_{C\sigma} + \hat{c}_{C\sigma}^\dagger \hat{c}_{A\sigma} + \hat{c}_{B\sigma}^\dagger \hat{c}_{C\sigma} + \hat{c}_{C\sigma}^\dagger \hat{c}_{B\sigma}) + t_{QQ}(\hat{c}_{A\sigma}^\dagger \hat{c}_{B\sigma} + \hat{c}_{B\sigma}^\dagger \hat{c}_{A\sigma})], \quad (21)$$

where $\hat{c}_{i\sigma}$ annihilates an electron with spin σ at site i .

2. Perturbation theory and reproduction of the Heisenberg spin Hamiltonian

Now we have G_0 and V , we can reproduce the Heisenberg Hamiltonian from the 2nd-, 3rd- and 4th-order perturbations to find the corresponding contributions to J_{QQ} and J_{CQ} according to the calculation procedure in §IV C:

$$J_{QQ} \simeq J_{QQ}^{(2)} + J_{QQ}^{(3)} + J_{QQ}^{(4)} \quad (22)$$

$$J_{CQ} \simeq J_{CQ}^{(2)} + J_{CQ}^{(3)} + J_{CQ}^{(4)}. \quad (23)$$

$J_{QQ}^{(i)}$, $J_{CQ}^{(i)}$, ($i = 2, 3, 4$) are functions of V_{QQ} , V_{CQ} , U_Q , U_C , t_{QQ} , and t_{CQ} ; all the contributions are given explic-

itly in Appendix B.

Motivated by the known physics of the defect problem, we choose suitable values for these variables to illustrate our results. We expect the hopping integrals t_{QQ} and t_{CQ} to decay exponentially with D_{QQ} and D_{CQ} respectively, at rates determined by the sum of the orbital exponents of the relevant atom pairs. We also expect $V_{QQ}, V_{CQ} < U_C < U_Q$ because the on-site Coulomb interaction should be larger than the Coulomb interaction between different centres, and the qubit spatial state is more localized than the control state.

For definiteness we take the following values for the parameters: $U_C = 1.0$, $U_Q = 1.5$, $V_{QQ} = 1/(2D_{QQ})$, $V_{CQ} = 1/(2D_{CQ})$, $t_{QQ} = -10^{-2}e^{-2/\nu_g D_{QQ}}$, $t_{CQ} = -e^{-(1/\nu_g + 1/\nu_c)D_{CQ}}$, $\nu_g = 0.7$, $\nu_c = 1.0$. Using these parameters, we calculate J_{CQ} , J_{QQ} shown in Figure (10).

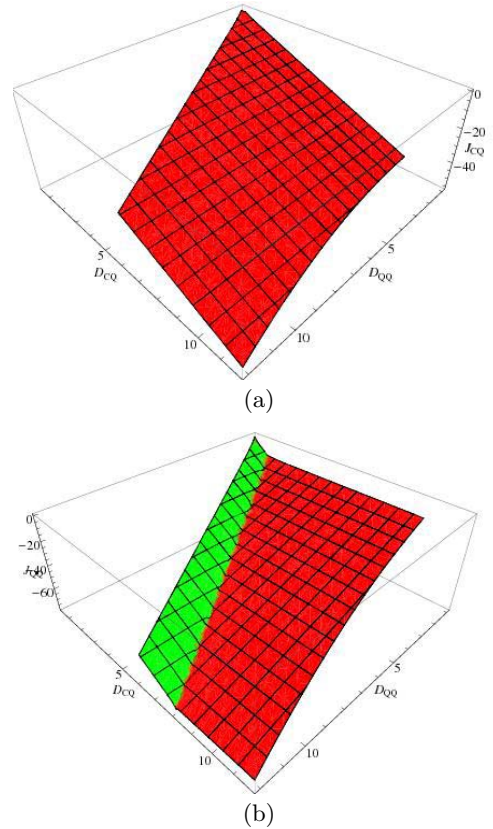


FIG. 10: (Colour online.) The exchange couplings (a) J_{CQ} and (b) J_{QQ} calculated by perturbation theory as a function of qubit distance D_{QQ} and qubit-control distance D_{CQ} . The sign of exchange coupling is coded in color; red: positive (antiferromagnetic) and green: negative (ferromagnetic). D_{QQ} varies from 1.0 to 12.0; H varies from 0 to 10.

Figure 10 shows us that when the qubit-qubit transfer amplitude t_{QQ} is much weaker than the control-qubit transfer t_{CQ} , ring-exchange will dominate over simple two-centre exchange and hence lead to ferromagnetic exchange couplings. The variations of exchange coupling shown in Figure 10 are qualitatively similar to those

shown in Figure 2(a) and Figure 3(a): when $D_{CQ} > D_{QQ}$, the exchange coupling is antiferromagnetic, while for some configurations where $D_{CQ} \ll D_{QQ}$ the exchange coupling is ferromagnetic. Note that in the values assumed for the parameters, the prefactor for t_{CQ} is chosen so that it is always much smaller than t_{CQ} ; we find that the magnitude of this prefactor tunes the boundary between the ferromagnetic and antiferromagnetic regions, as might be expected because of its effect on the relative magnitudes of third- and fourth-order processes. For the excited control, t_{CQ} is larger and the ferromagnetic region is consequently further extended. Ultimately with these parameters a negative (ferromagnetic) part in the qubit-qubit exchange coupling J_{QQ} arises at intermediate qubit-control separations.

V. STATISTICAL DISTRIBUTION OF EXCHANGE INTERACTIONS

Since there is a strong configuration dependence of the exchange interactions it is natural to ask about their probability distributions at given impurity concentrations, since these distributions will determine the system's response to macroscopic, spatially averaging, probes. We proceed as follows: we define a cluster of three spins to consist of a qubit atom, its nearest-neighbour qubit atom, and the control atom nearest to their mid-point. Then, assuming the qubits and controls are independently and uniformly distributed (i.e. neglecting both defect-defect correlations and the underlying lattice structure), the probability $P(D_{CQ}, H) dD_{CQ} dH$ that the qubit-qubit distance is between D_{CQ} and $D_{CQ} + dD_{CQ}$ while the control's distance from the mid-point is between H and $H + dH$, is given by a simple generalization of the argument of Chandrasekhar [39] as

$$P(D_{CQ}, H) = 16\pi^2 D_{CQ}^2 H^2 n_Q n_C e^{-\frac{4\pi}{3}(n_Q D_{CQ}^3 + n_C H^3)}, \quad (24)$$

where n_Q and n_C are the volume densities of qubit and control atoms respectively. For purely exponential interactions between defect pairs, the averages over this type of distribution may be performed analytically [40]; since we know that in this case the interactions depend on both D_{CQ} and H , and are not purely exponential, we must resort to a numerical average.

Our key approximation is to assume that the exchange couplings computed in §III (i.e., in an isosceles configuration with both qubit-control distances equal) are representative of all configurations with the same values of D_{CQ} and H ; we suspect that this approximation will lead to excessive delocalization of the control electron and hence to an over-estimate of the exchange. We compute the induced distribution of exchange couplings from our previous results by summing over the same mesh used to generate Figures 2 and 3, accumulating a suitably weighted histogram of exchange values by convoluting the delta-function contributions from each calculated

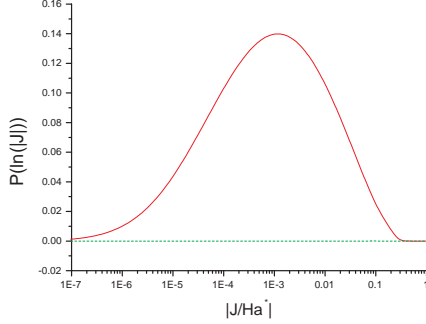
point with a Gaussian whose width is chosen to produce a smooth curve without introducing excessive broadening. At the densities chosen, this mesh accounts for approximately 98% of the normalization of $P(D_{CQ}, H)$. The results are shown in Figures (11) and (12), in the form of distribution functions for $\log |J|$ with the contributions from positive and negative J (i.e. antiferromagnetic and ferromagnetic parts) displayed separately. From Figure 11(a), we can see that when the control is in the ground state the distribution of qubit-control exchange is overwhelmingly antiferromagnetic and qualitatively similar to those calculated for defect pairs of similar binding energies at comparable densities [17]. However, when the control is excited (Figure 11(b)) the antiferromagnetic distribution narrows dramatically and shifts to higher $|J|$, both because of the slower decay with distance and because of the significant ferromagnetic region discussed in §III. At the same time the ferromagnetic part to the distribution grows.

Similarly, when the control is in the ground state the distribution of J_{QQ} (Figure 12) is predominantly antiferromagnetic and very close to that for deep-donor pairs at the same density [17]. The small ferromagnetic part is due to the ring exchange described in §IV. When the control is excited, this ferromagnetic region is greatly enlarged owing to the enhanced t_{CQ} , which leads to ring exchange dominating the two-donor exchange as illustrated in §IV.

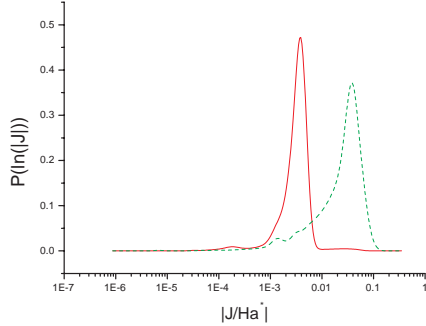
VI. DISCUSSION AND CONCLUSION

We have described a variational method for calculating the exchange interactions between three electrons in a control-qubit system of the type envisaged for optically-controlled quantum information processing in silicon [6]. We have deliberately kept the model simple, yet rich enough to capture the coupling of the changing electron distribution to the spin configuration as the geometry and degree of excitation are altered.

The principal conclusion is that a three-centre system such as this is significantly different from the sum of two-electron exchange interactions that would arise from considering each defect pair separately. In particular the excitation of the control electron can alter the 'qubit-qubit' coupling J_{QQ} as well as the 'control-qubit' coupling J_{CQ} . This is partly because of the delocalization of the electronic states across all three centres (particularly when the control electron is in an excited state), and partly because of the presence of three-centre ring-exchange processes (which we have also described perturbatively). Most strikingly, we predict that either or both the control-qubit coupling J_{CQ} and the qubit-qubit coupling J_{QQ} can become ferromagnetic; this can happen through either of the above mechanisms. The excitation of the control greatly enhances both the ferromagnetism and the degree of charge transfer; however, it is interesting that J_{CQ} can be ferromagnetic even when the control



(a)

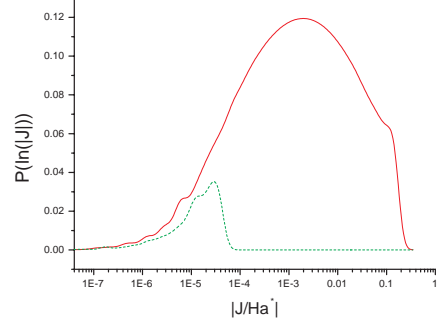


(b)

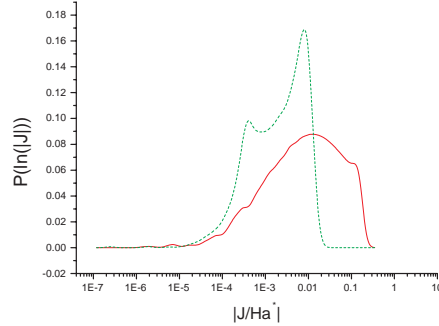
FIG. 11: (Colour online.) The probability distribution of $\log |J_{CQ}|$ for the control-qubit coupling, shown as a function of J_{CQ} (on a logarithmic scale) for the control atom in (a) its ground state and (b) its excited state. Red solid curve: distribution of antiferromagnetic couplings; green dashed curve: ferromagnetic couplings. The density of qubit atoms was taken as $0.00396 (a_0^*)^{-3} = 5.42 \times 10^{17} \text{ cm}^{-3}$, and the density of control atoms as $0.00198 (a_0^*)^{-3} = 2.71 \times 10^{17} \text{ cm}^{-3}$. The plot was constructed by sampling over the 111×101 -point grid used to create Figure 2, smoothed by convolving each point with a Gaussian in $\log |J_{CQ}|$ of standard deviation 0.224.

is in the ground state. The qualitative agreement between our variational results and those of the simple perturbation theory (which includes only the ring-exchange mechanism) shows that the latter is especially important when the control is in the ground state. The ferromagnetic couplings we predict could be exploited for the initialization or manipulation of donor spins.

As might be expected, when the control electron moves further away, J_{QQ} returns to the value expected for a deep donor pair without any control species [17]. This is also reflected in the statistical distributions of exchange values, where the distribution of J_{QQ} with the control in the ground state is quite similar to the exchange distribution for deep-donor pairs calculated in [17]. However, when the control electron is located between the two qubits the magnitude of J_{QQ} increases significantly, owing to the mediation by the control electron; this is es-



(a)



(b)

FIG. 12: (Colour online.) The probability distribution of $\log |J_{QQ}|$ for the qubit-qubit coupling as a function of J_{QQ} (on logarithmic scale) for the control atom in (a) the ground state and (b) the excited state. Red solid curve: distribution of antiferromagnetic couplings; green dashed curve: ferromagnetic coupling distribution. The parameters used to construct the plot were as for Figure 11.

pecially significant when the qubit-qubit distance is large. In this limit J_{QQ} can also become ferromagnetic, because the fourth-order terms containing t_{CQ} which give a ferromagnetic contribution dominate. When the qubit-qubit distance is relatively small, the second-order terms involving t_{QQ} dominate J_{QQ} , and the control electron is a minor perturbation on the two-qubit sub-system.

Our results show that the process of excitation and de-excitation can produce substantial but quite complex changes in the exchange couplings and charge distributions in these model defect complexes. They provide a theoretical demonstration of the switching of exchange couplings by excitation; a quantitative understanding of this process will have implications both for optically-controlled magnetism in silicon, and for quantum computation.

Acknowledgments

We wish to acknowledge the support of the UK Research Councils Basic Technology Programme under

grant GR/S23506. We thank Gabriel Aeppli, Tony Harker, Andy Kerridge, Chiranjib Mitra, Marshall Stoneham, and Dan Wheatley for helpful discussions.

APPENDIX A: COMPUTING THE COEFFICIENTS IN THE SPIN HAMILTONIAN

Equation (15) is the most general rotationally-invariant three-spin Hamiltonian that is even under time reversal. Total spin angular momentum is a good quantum number, and standard angular momentum coupling schemes [38] show that three spin-1/2 particles can be coupled to a quartet $|Q\rangle = \{[\frac{1}{2}, \frac{1}{2}]_1, \frac{1}{2}\}_{\frac{3}{2}}$, and to two different doublets, $|D_L\rangle = \{[\frac{1}{2}, \frac{1}{2}]_L, \frac{1}{2}\}_{\frac{1}{2}}$ distinguished

by the intermediate angular momentum L , which can be 0 or 1.

Since the full spin Hamiltonian (15) is traceless, we may conveniently write its eigenvalues as

$$\begin{aligned} E_{D_0} &= -\epsilon - \delta/2 && \text{(doublet)} \\ E_{D_1} &= -\epsilon + \delta/2 && \text{(doublet)} \\ E_Q &= \epsilon && \text{(quartet)} \end{aligned} \quad (\text{A1})$$

It is sufficient to work with the three states having total spin component 1/2 ($|001\rangle$, $|010\rangle$ and $|100\rangle$); they are only coupled amongst themselves, and within this subspace the Hamiltonian is

$$\frac{1}{4} \begin{bmatrix} J_{CQB} - J_{CQA} - J_{QQ} & 2J_{QQ} & 2J_{CQA} \\ 2J_{QQ} & -J_{CQB} + J_{CQA} - J_{QQ} & 2J_{CQB} \\ 2J_{CQA} & 2J_{CQB} & -J_{CQB} - J_{CQA} + J_{QQ} \end{bmatrix} \quad (\text{A2})$$

which has one eigenvalue

$$\frac{J_{QQ} + J_{CQA} + J_{CQB}}{4} = E_Q, \quad (\text{A3})$$

(corresponding to the component of the quartet with magnetic quantum number=1/2), while the other two eigenvalues are

$$-\epsilon \pm \frac{1}{2} \sqrt{(J_{CQB}^2 + J_{CQA}^2 + J_{QQ}^2) - J_{CQA}J_{QQ} - J_{QQ}J_{CQB} - J_{CQB}J_{CQA}} \quad (\text{A4})$$

(corresponding to the two doublet states).

Now, in the symmetric case $J_{CQA} = J_{CQB} = J_{CQ}$, it is straightforward to show that

$$\mathcal{L} = \langle (s_A + s_B)^2 \rangle \quad (\text{A5})$$

commutes with the Hamiltonian. Since \mathcal{L} is the operator which corresponds to the intermediate angular momentum L described above, we may characterize the two doublet states by their intermediate L value. Once more it is convenient to work within the spin 1/2 subspace, where a short calculation shows that the doublet state with $L = 0$ has the eigenvector $\{1, -1, 0\}^T/\sqrt{2}$, with eigenvalue

$$E_{D_0} = -\frac{3J_{QQ}}{4}, \quad (\text{A6})$$

whereas the doublet characterized by $L = 1$ has eigenvalue

$$E_{D_1} = \frac{J_{QQ}}{4} - J_{CQ} \quad (\text{A7})$$

with eigenvector $\{1, 1, -2\}^T/\sqrt{6}$. The quartet state, of course has eigenvalue

$$E_Q = \frac{J_{CQ}}{2} + \frac{J_{QQ}}{4}, \quad (\text{A8})$$

and eigenvector $\{1, 1, 1\}^T/\sqrt{3}$. Thus, the simplest way of determining the exchange parameters J_{QQ} and J_{CQ} is to identify the doublet state with $L = 0$ and the quartet state and use the relations (16) given in the main text.

Notice it is important to identify the doublet states by their wavefunction; their energies alone are not sufficient. The *eigenvalues* of the Hamiltonian defined by the exchange parameters J_{CQ} and J_{QQ} are identical to those of the Hamiltonian obtained by the substitutions

$$\begin{aligned} J_{CQ} &\rightarrow \frac{1}{3}(J_{CQ} + 2J_{QQ}); \\ J_{QQ} &\rightarrow \frac{1}{3}(4J_{CQ} - J_{QQ}). \end{aligned} \quad (\text{A9})$$

However, the *eigenvectors* of the doublets interchange their properties under this substitution. This is related to the sign ambiguity in the square root in equation A3, which makes the sign of δ in A1 ambiguous.

APPENDIX B: ANALYTIC RESULTS FROM
PERTURBATION THEORY

The lowest-order (second-order) contributions to the exchange are

$$J_{CQ}^{(2)} = -\frac{2t_{CQ}^2}{-U_Q + 2V_{CQ} - V_{QQ}} - \frac{2t_{CQ}^2}{V_{QQ} - U_C}; \quad (\text{B1})$$

$$J_{QQ}^{(2)} = -\frac{4t_{QQ}^2}{V_{QQ} - U_Q}. \quad (\text{B2})$$

The third-order contributions are

$$J_{CQ}^{(3)} = \frac{2t_{CQ}^2 t_{QQ}}{(V_{QQ} - U_C)^2} - \frac{2t_{CQ}^2 t_{QQ}}{(-U_Q + 2V_{CQ} - V_{QQ})^2}; \quad (\text{B3})$$

$$J_{QQ}^{(3)} = \frac{4t_{QQ} t_{CQ}^2}{(-U_Q + 2V_{CQ} - V_{QQ})(V_{QQ} - U_Q)} - \frac{4t_{QQ} t_{CQ}^2}{(V_{QQ} - U_C)(V_{QQ} - U_Q)} \quad (\text{B4})$$

$$+ \frac{2t_{QQ} t_{CQ}^2}{(-U_Q + 2V_{CQ} - V_{QQ})^2} - \frac{2t_{QQ} t_{CQ}^2}{(V_{QQ} - U_C)^2},$$

while the fourth-order terms are

$$J_{CQ}^{(4)} = -\frac{4t_{CQ}^4}{(-U_Q + 2V_{CQ} - V_{QQ})(V_{QQ} - U_C)(V_{QQ} - U_Q)} - \frac{2t_{CQ}^4}{(-U_Q + 2V_{CQ} - V_{QQ})^2(V_{QQ} - U_Q)} \quad (\text{B5})$$

$$- \frac{2t_{CQ}^4}{(V_{QQ} - U_C)^2(V_{QQ} - U_Q)} - \frac{2t_{QQ}^2 t_{CQ}^2}{(-U_Q + 2V_{CQ} - V_{QQ})^3} - \frac{2t_{QQ}^2 t_{CQ}^2}{(V_{QQ} - U_C)^3};$$

$$J_{QQ}^{(4)} = \frac{4t_{CQ}^4}{(-U_Q + 2V_{CQ} - V_{QQ})(V_{QQ} - U_C)(V_{QQ} - U_Q)} - \frac{4t_{QQ}^2 t_{CQ}^2}{(-U_Q + 2V_{CQ} - V_{QQ})^2(V_{QQ} - U_Q)} \quad (\text{B6})$$

$$- \frac{4t_{QQ}^2 t_{CQ}^2}{(V_{QQ} - U_C)^2(V_{QQ} - U_Q)} - \frac{4t_{QQ}^2 t_{CQ}^2}{(-U_Q + 2V_{CQ} - V_{QQ})(V_{QQ} - U_Q)^2} - \frac{4t_{QQ}^2 t_{CQ}^2}{(V_{QQ} - U_C)(V_{QQ} - U_Q)^2}.$$

-
- [1] Kane, B. Nature **393** 133 (1998).
[2] B. Koiller, *et al.*, Phys. Rev. Lett. **88** 027903 (2001).
[3] T. G. Castner, Jr., Phys. Rev. **130** 58 (1963).
[4] S. R. Schofield, N. J. Curson, M. Y. Simmons, *et al.*, Phys. Rev. Lett. **91** 136104 (2003)
[5] Jamieson DN, Yang C, Hopf T, *et al.*, App. Phys. Lett. **86** 202101 (2005).
[6] A.M.Stoneham, A.J.Fisher and P.T.Greenland, J. Phys.: Condensed Matter **15** L447 (2003).
[7] A.M.Stoneham, *Theory of Defects in Solids (Oxford University Press, 1975)*.
[8] N.Itoh and A.M.Stoneham, *Materials Modification by Electronic Excitation (Cambridge University Press, 2001)*.
[9] C. Piermarocchi, Pochung Chen, L. J. Sham, and D. G. Steel, Phys. Rev. Lett. **89** 167402 (2002).
[10] R. Rodriguez, A.J. Fisher, P.T. Greenland and A.M .Stoneham. J. Phys.: Condens. Matt. **16** 2757-2772 (2004).
[11] C. Herring and M. Flicker, Phys. Rev. **134** A632 (1962).
[12] P. R. Cullis and J. R. Marko, Phys. Rev. B **1** 632 (1970).
[13] K. Andres, R. N. Bhatt, P. Goalwin, *et al.*, Phys. Rev. B **24** 244 (1981).
[14] B. Koiller, *et al.*, Phys. Rev. B **66** 115201 (2002).
[15] C. J. Wellard, L. C. L. Hollenberg, F. Parisoli, *et al.*, Phys. Rev. B **68** 195209 (2003).
[16] B. Koiller, R. B. Capaz, Xuedong Hu, *et al.*, Phys. Rev. B **70** 115207 (2004).

- [17] W. Wu and A. J. Fisher, arXiv: 0709.0268 (2007).
- [18] C. Timm, F. Schäfer, and F. von Oppen, Phys. Rev. Lett. **89** 137201 (2002).
- [19] M. Roger, J. H. Hetherington, and J. M. Delrieu, Rev. Mod. Phys. **55** 1.
- [20] Ari Mizel and Daniel A. Lidar, Phys. Rev. Lett. **92** 077903 (2004).
- [21] Ari Mizel and Daniel A. Lidar, Phys. Rev. B **70** 115310 (2004).
- [22] R. Woodworth, A. Mizel, DA Lidar, J. Phys.: Condens. Matter **18** S721 (2006).
- [23] V. W. Scarola and S. Das Sarma, Phys. Rev. A **71** 032340 (2005).
- [24] W. Heitler and F. London, Z. Phys. **44** 455 (1927).
- [25] John C. Slater, *Quantum theory of molecules and solids*, (McGraw-Hill,1963).
- [26] N. Q. Vinh, P. T. Greenland, K. Litvinenko *et al.* ‘Silicon as the ultimate ion trap: time-domain measurements of donor Rydberg states’. To be submitted to *Nature Physics*.
- [27] Luttinger J. M. and Kohn W., Phys. Rev. **97** 869 (1955).
- [28] Luttinger J. M. and Kohn W., Phys. Rev. **98** 915 (1955).
- [29] R. A. Faulkner Phys. Rev. **184** 713 (1969).
- [30] H. Barry Bebb, J. Phys. Chem. Solids, **28** 2087 (1967).
- [31] H. Nara and A. Morita, J. Phys. Soc. Jpn. **21** 1852 (1966).
- [32] H. Nara and A. Morita, J. Phys. Soc. Jpn. **23** 831 (1967).
- [33] A. Kerridge, S. Savory, A. H. Harker and A. M. Stoneham, J. Phys.: Condens. Mat. **18** S767-S776 (2006).
- [34] Heisenberg, W Z.Phys. **49** 619 (1928).
- [35] P. W. Anderson, Phys. Rev. **115** 2 (1959).
- [36] M. Abramowitz and I.A. Stegun, *Handbook of Mathematical Functions*, Dover Publications (1965).
- [37] G. K. Woodgate *Elementary Atomic Structure*, Oxford University Press (1983)
- [38] A. R. Edmonds ‘Angular Momentum in Quantum Mechanics’, Princeton University Press, (Princeton, New Jersey) 1957.
- [39] S. Chandrasekhar, Rev. Mod. Phys. **15**, 1 (1943).
- [40] A.M. Stoneham, J.Phys. C **16**, 285 (1983).